

Prediction of the Effect of Single Amino Acid Protein Variants Using Deep Mutational Scanning Data

University of Bologna — Master Thesis in Bioinformatics

Pierotti Saul

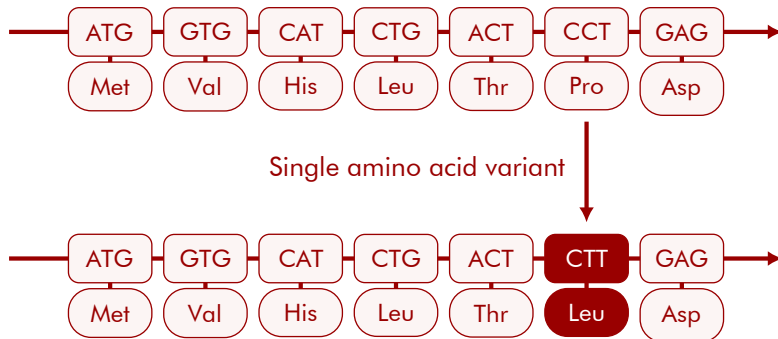
Internal Advisor: Prof. Pietro Di Lena

External Advisor: Prof. Arne Elofsson (Stockholm University)

July 19, 2021

Single Amino Acid Variant

A mutation that replaces exactly one amino acid in a protein



Deep Mutational Scanning

A technique for obtaining fitness information on a large number of mutations

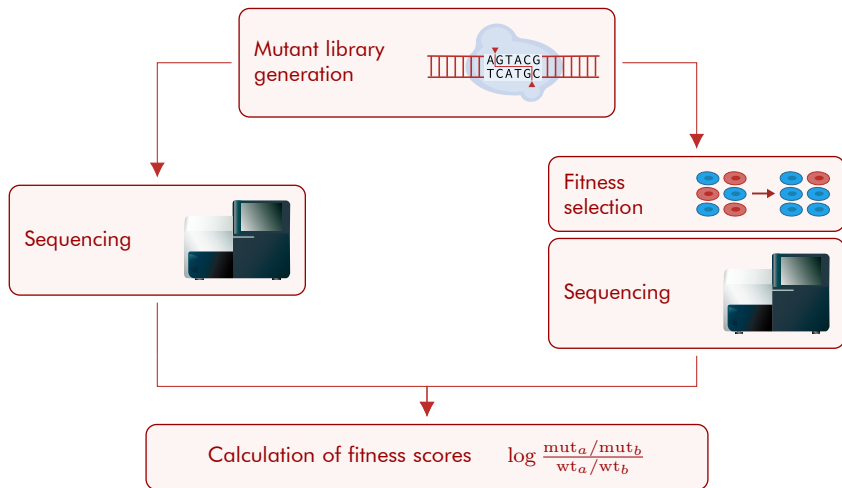
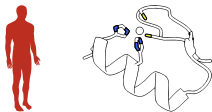


Image sources: restriction_enzyme icon by Simon Dürri; Illumina_miseq icon by DBCLS; modification of stem_cell_colony icon by Marcel Tisch. Full credits in appendix.

Predicting the Effect of Mutations

Why is it useful?

- ▶ Targeted medical treatments
- ▶ Protein engineering



Why is it needed?

- ▶ Experiments are insufficient
- ▶ Experiments are expensive



How can it be done?

- ▶ Machine learning
- ▶ Statistical models

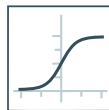
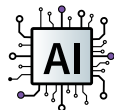


Image sources: modification of patient icon by Marcel Tisch; zincfinger icon by Simon Dür; Illumina_miseq icon by DBCLS; sand-clock icon by Servier; ai icon by Simon Dür; sigmoid icon by Simon Dür. Full credits in appendix.

Previous Work in the Field

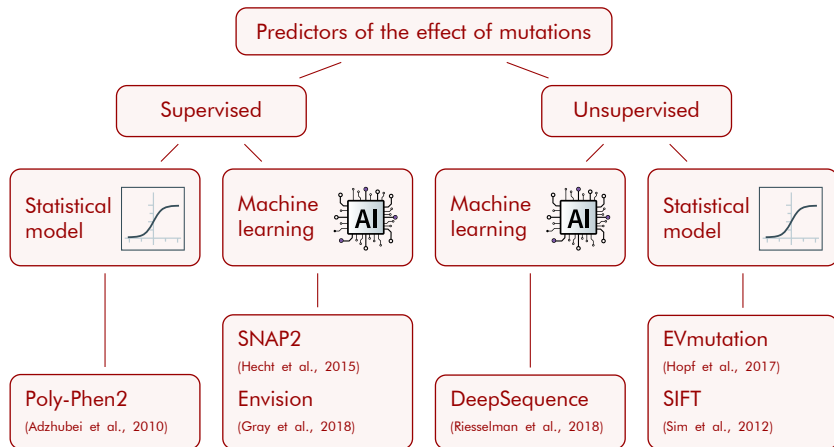
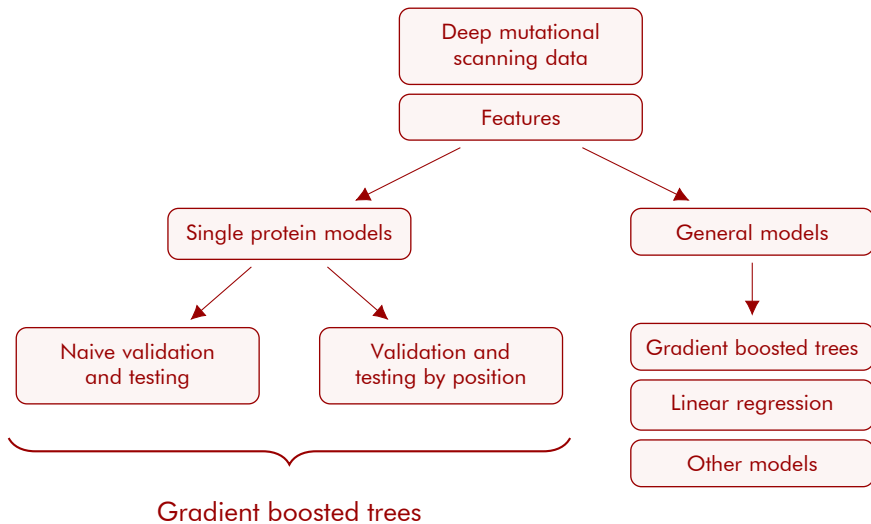


Image sources: ai icon by Simon Dürr; sigmoid icon by Simon Dürr. Full credits in appendix.

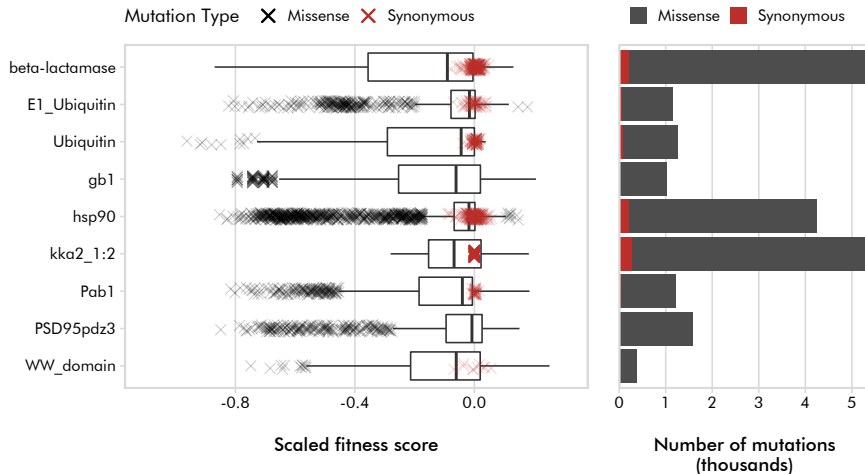
Among these predictors only Envision was trained on deep mutational scanning data

My Approach



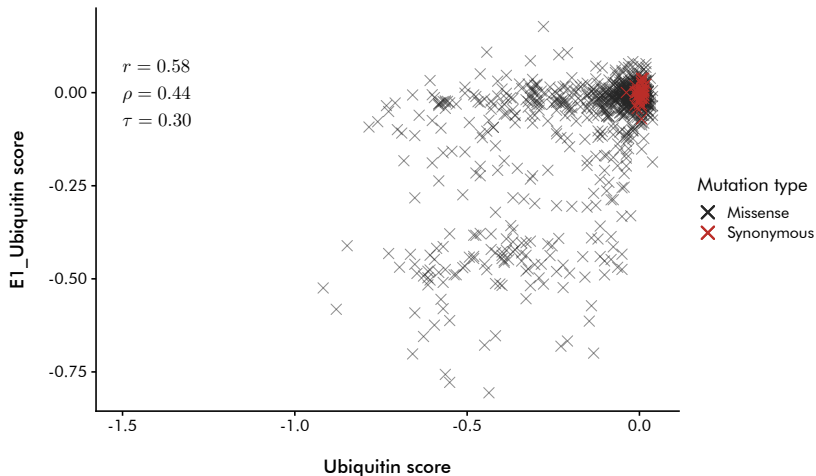
Training Data

I borrowed the training dataset of the predictor Envision (Gray et al., 2018)

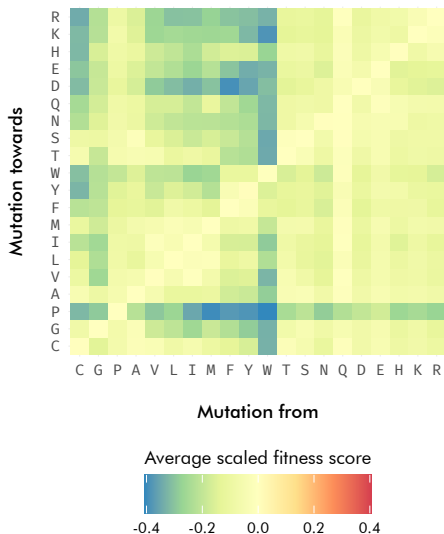


Experiments Do Not Agree Much with Each Other

Two independent deep mutational scanning experiments on Ubiquitin are present in the training dataset. Their correlation is low.



Interesting Patterns in Mutation Sensitivity

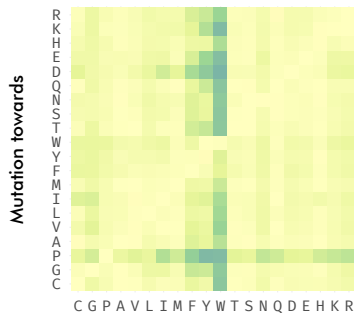


- ▶ Polar residues seem more tolerant to mutations than hydrophobic residues
- ▶ Proline (P) is the most disruptive residue
- ▶ Tryptophan (W) is hard to replace

Exposure Explains the Mutability of Polar Residues

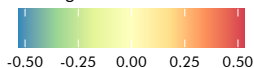
When filtering by Relative Solvent Accessibility (RSA) apolar residues are **not** more sensitive to mutations than polar residues

Exposed positions (RSA > 0.15)

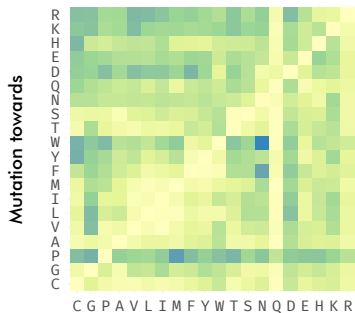


Mutation from

Average scaled fitness score

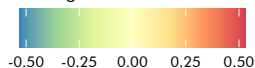


Buried positions (RSA ≤ 0.15)

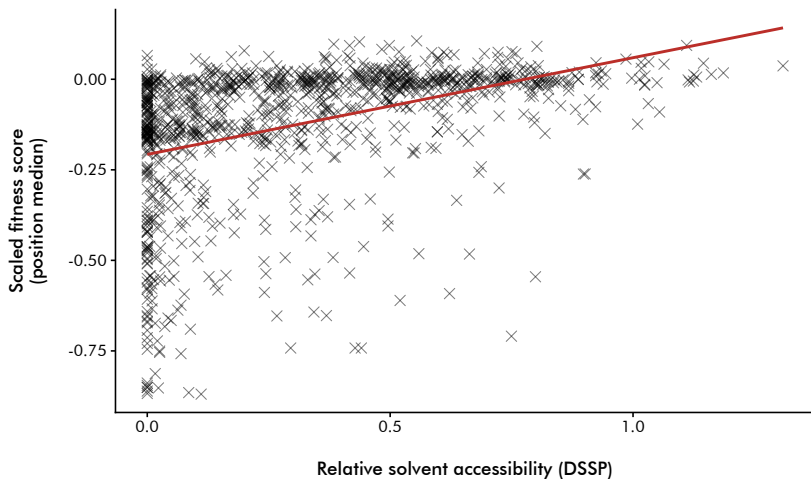


Mutation from

Average scaled fitness score



Buried Residues Are More Conserved



Features Used by the Predictors

All the features are derived from the sequences: I did **not** use any structural information

Mutation identity

Ser → Thr

EVmutation predictions

(Hopf et al., 2017)



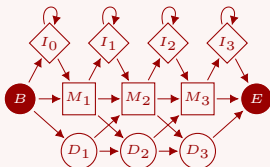
NetsurfP-2 predictions

(Klausen et al., 2019)



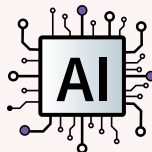
HMMER emission probabilities

(Eddy, 2011)

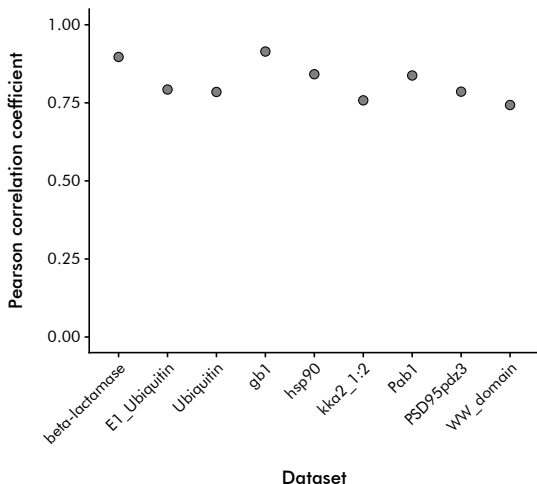


trRosetta predicted contacts

(Yang et al., 2020)



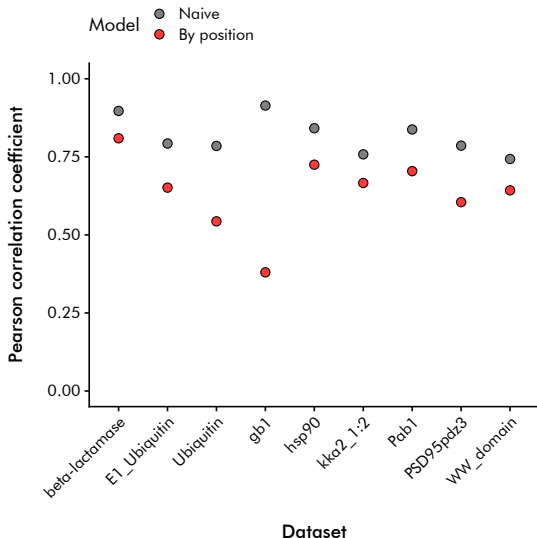
Single Protein Models



Naive approach

- ▶ A different model trained for each protein
- ▶ Half of the mutations used for testing and half for cross-validation
- ▶ Too good to be true

Single Protein Models



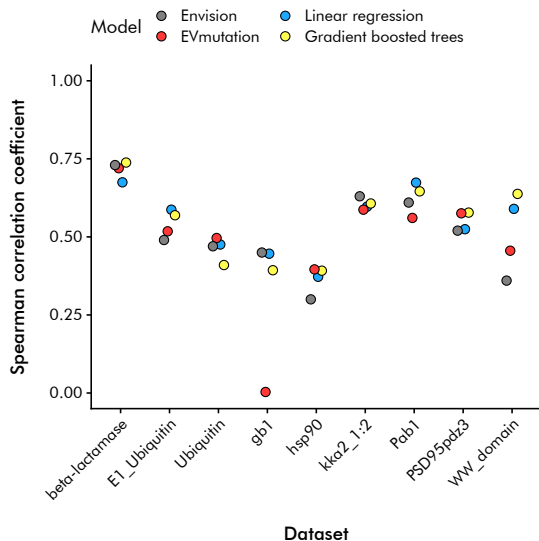
Naive approach

- ▶ A different model trained for each protein
- ▶ Half of the mutations used for testing and half for cross-validation
- ▶ Too good to be true

Segregating protein positions

- ▶ Same as above but mutations in the same position segregated in the training or testing sets
- ▶ Performances are more realistic

Leave-One-Protein-Out (LOPO) Models



- ▶ Models trained on the whole dataset while leaving one protein out
- ▶ For the left-out protein, half of the mutations used for testing and half for validation
- ▶ Spearman correlation coefficient used for evaluation

What I learned

- ▶ The testing strategy is crucial
- ▶ Good performances without structural features
- ▶ Strong variability between datasets
- ▶ Complex models not necessarily better



Ideas for the future

- ▶ Using residue contacts in a graph convolutional neural network
- ▶ Training on more deep mutational scanning studies
- ▶ Finding a better normalization strategy



Image sources: personal creation; hell-birne-karriere-klettern-licht by mohamed_hassan. Full credits in appendix.

Questions?



Image sources: hombre-pensamiento-silueta-4484226 by mohamed_hassan. Full credits in appendix.

Bibliography I

- Adzhubei, I. A., Schmidt, S., Peshkin, L., Ramensky, V. E., Gerasimova, A., Bork, P., Kondrashov, A. S. & Sunyaev, S. R. (2010). A method and server for predicting damaging missense mutations. *Nature Methods*, 7(4), 248–249. <https://doi.org/10.1038/nmeth0410-248>
- Eddy, S. R. (2011). Accelerated profile HMM searches (W. R. Pearson, Ed.). *PLoS Computational Biology*, 7(10), e1002195. <https://doi.org/10.1371/journal.pcbi.1002195>
- Gray, V. E., Hause, R. J., Luebeck, J., Shendure, J. & Fowler, D. M. (2018). Quantitative missense variant effect prediction using large-scale mutagenesis data. *Cell Systems*, 6(1), 116–124.e3. <https://doi.org/10.1016/j.cels.2017.11.003>
- Hecht, M., Bromberg, Y. & Rost, B. (2015). Better prediction of functional effects for sequence variants. *BMC Genomics*, 16(S8). <https://doi.org/10.1186/1471-2164-16-s8-s1>
- Hopf, T., Ingraham, J., Poelwijk, F., Schärfe, C., Springer, M., Sander, C. & Marks, D. (2017). Mutation effects predicted from sequence co-variation. *Nature Biotechnology*, 35(2), 128–135. <https://doi.org/10.1038/nbt.3769>

Bibliography II

- Klausen, M. S., Jespersen, M. C., Nielsen, H., Jensen, K. K., Jurtz, V. I., Sønderby, C. K., Sommer, M. O. A., Winther, O., Nielsen, M., Petersen, B. & Marcatili, P. (2019). NetSurfP-2.0: Improved prediction of protein structural features by integrated deep learning. *Proteins: Structure, Function, and Bioinformatics*, 87(6), 520–527. <https://doi.org/10.1002/prot.25674>
- Riesselman, A. J., Ingraham, J. B. & Marks, D. S. (2018). Deep generative models of genetic variation capture the effects of mutations. *Nature Methods*, 15(10), 816–822. <https://doi.org/10.1038/s41592-018-0138-4>
- Sim, N.-I., Kumar, P., Hu, J., Henikoff, S., Schneider, G. & Ng, P. C. (2012). SIFT web server: Predicting effects of amino acid substitutions on proteins. *Nucleic Acids Research*, 40(W1), W452–W457. <https://doi.org/10.1093/nar/gks539>
- Yang, J., Anishchenko, I., Park, H., Peng, Z., Ovchinnikov, S. & Baker, D. (2020). Improved protein structure prediction using predicted interresidue orientations. *Proceedings of the National Academy of Sciences*, 117(3), 1496–1503. <https://doi.org/10.1073/pnas.1914677117>

Images Credits

llumina_miseq icon by DBCLS <https://togotv.dbcls.jp/en/pics.html> is licensed under CC-BY 4.0 Unported <https://creativecommons.org/licenses/by/4.0/>

restriction_enzyme icon by Simon Dürr <https://twitter.com/simondueerr> is licensed under CC0 <https://creativecommons.org/publicdomain/zero/1.0/>

zincfinger icon by Simon Dürr <https://twitter.com/simondueerr> is licensed under CC0 <https://creativecommons.org/publicdomain/zero/1.0/>

stem_cell_colony icon by Marcel Tisch <https://twitter.com/MarcelTisch> is licensed under CC0 <https://creativecommons.org/publicdomain/zero/1.0/>

ai icon by Simon Dürr <https://twitter.com/simondueerr> is licensed under CC0 <https://creativecommons.org/publicdomain/zero/1.0/>

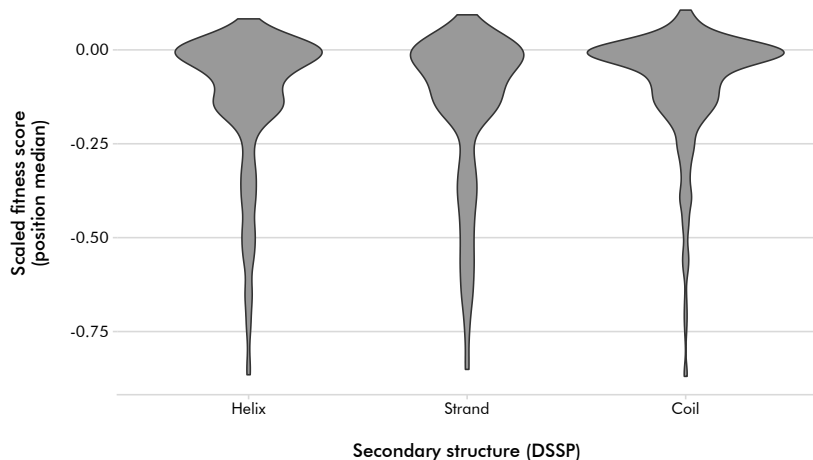
sigmoid icon by Simon Dürr <https://twitter.com/simondueerr> is licensed under CC0 <https://creativecommons.org/publicdomain/zero/1.0/>

hombre-pensamiento-silueta by mohamed_hassan <https://pixabay.com/es/vectors/hombre-pensamiento-silueta-4484226/> is licensed under Simplified Pixabay License <https://pixabay.com/service/terms/#license>

hell-birne-karriere-klettern-licht by mohamed_hassan <https://pixabay.com/de/vectors/hell-birne-karriere-klettern-licht-2855120/> is licensed under Simplified Pixabay License <https://pixabay.com/service/terms/#license>

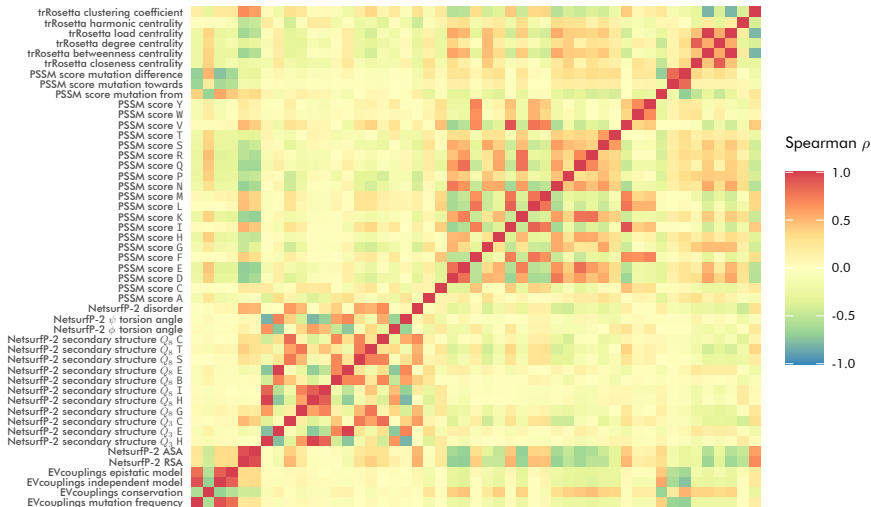
Supplementary Material

Secondary structure is of limited importance in the discrimination of damaging mutations



Supplementary Material

The correlation among features follows predictable patterns



Supplementary Material

Precision of trRosetta (Yang et al., 2020) in predicting residue contacts

Dataset	Medium-range ($s \geq 12$)			Long-range ($s \geq 24$)		
	Top $L/5$	Top $L/2$	Top L	Top $L/5$	Top $L/2$	Top L
beta-lactamase	1.00	0.92	0.86	0.96	0.93	0.76
WW_domain	0.95	0.90	0.83	0.90	0.87	0.75
PSD95pdz3	0.96	0.92	0.80	0.92	0.81	0.70
kka2_1:2	1.00	1.00	0.96	1.00	1.00	0.89
hsp90	1.00	1.00	0.96	1.00	1.00	0.89
Ubiquitin	0.98	0.92	0.82	1.00	0.90	0.70
Pab1	0.80	0.72	0.67	0.87	0.74	0.60
E1_Ubiquitin	0.82	0.86	0.77	0.91	0.75	0.54
gb1	1.00	0.85	0.46	0.63	0.40	0.22

Quality of the predicted structural features from NetsurfP-2 (Klausen et al., 2019)

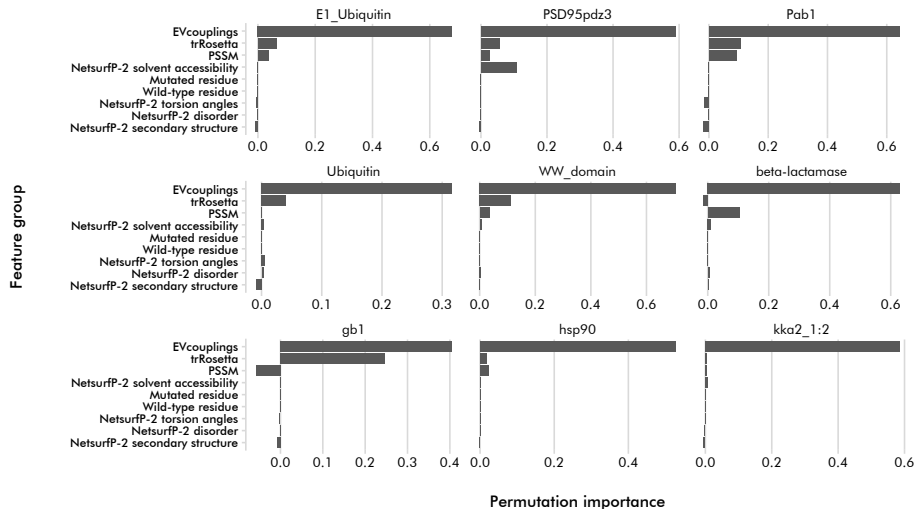
Feature	Evaluation metric	Score
Relative solvent accessibility	Pearson r	0.79
Accessible surface area	Pearson r	0.80
Q_3 secondary structure	Q_3 accuracy	0.85
Q_8 secondary structure	Q_8 accuracy	0.72
ϕ torsion angle	Circular correlation	0.73
ψ torsion angle	Circular correlation	0.87

Relationship between the features used in the models and the fitness scores

Feature	Pearson r	Spearman ρ	Kendall τ
PSSM mutation score	-0.29	-0.28	-0.19
Netsurf predicted RSA	0.34	0.37	0.25
Netsurf predicted ASA	0.32	0.35	0.24
Netsurf predicted disorder	0.06	0.18	0.12
EVcouplings epistatic model	0.46	0.50	0.34
EVcouplings independent model	0.44	0.44	0.30
EVcouplings frequency	0.19	0.35	0.24
EVcouplings conservation	-0.32	-0.33	-0.23
Closeness centrality (trRosetta predicted contacts)	-0.16	-0.17	-0.11
Betweenness centrality (trRosetta predicted contacts)	-0.20	-0.29	-0.19
Degree centrality (trRosetta predicted contacts)	-0.12	-0.13	-0.09
Load centrality (trRosetta predicted contacts)	-0.20	-0.29	-0.19
Harmonic centrality (trRosetta predicted contacts)	-0.19	-0.20	-0.14
Clustering coefficient (trRosetta predicted contacts)	0.23	0.25	0.17
Linear-circular correlation			
Netsurf predicted ϕ torsion angle			0.01
Netsurf predicted ψ torsion angle			0.02
	Kruskal-Wallis χ^2	p -value	
Wild-type residue	1482.40	$< 2.20 \cdot 10^{-16}$	
Mutated residue	708.53	$< 2.20 \cdot 10^{-16}$	
Netsurf predicted Q_3 secondary structure	215.33	$< 2.20 \cdot 10^{-16}$	
Netsurf predicted Q_8 secondary structure	351.97	$< 2.20 \cdot 10^{-16}$	

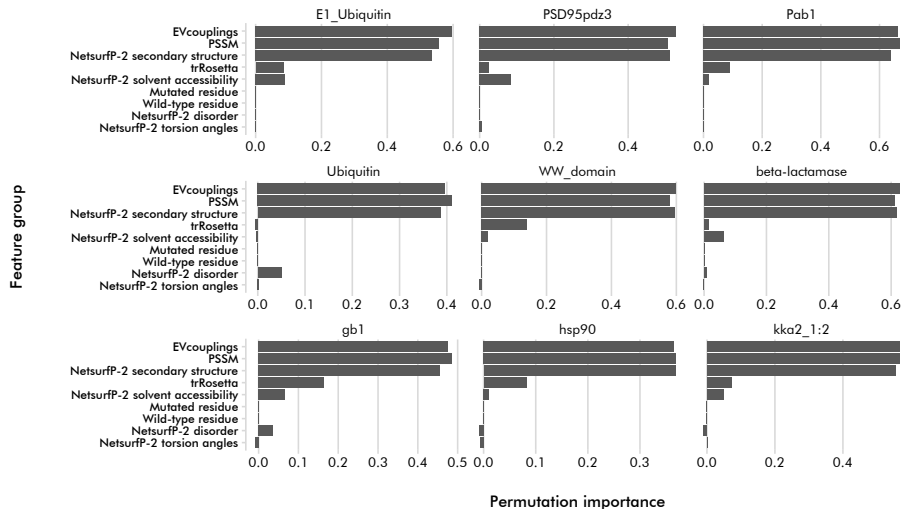
Supplementary Material

Feature importances for the gradient boosted tree general models



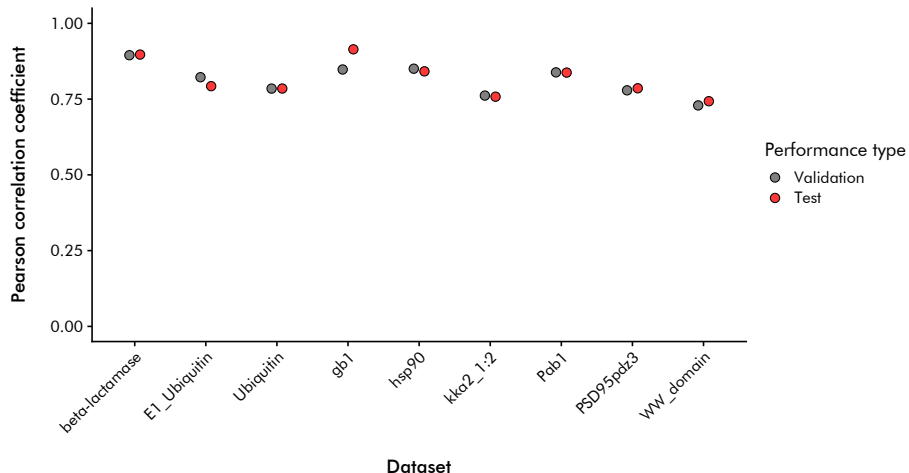
Supplementary Material

Feature importances for the linear regression general models



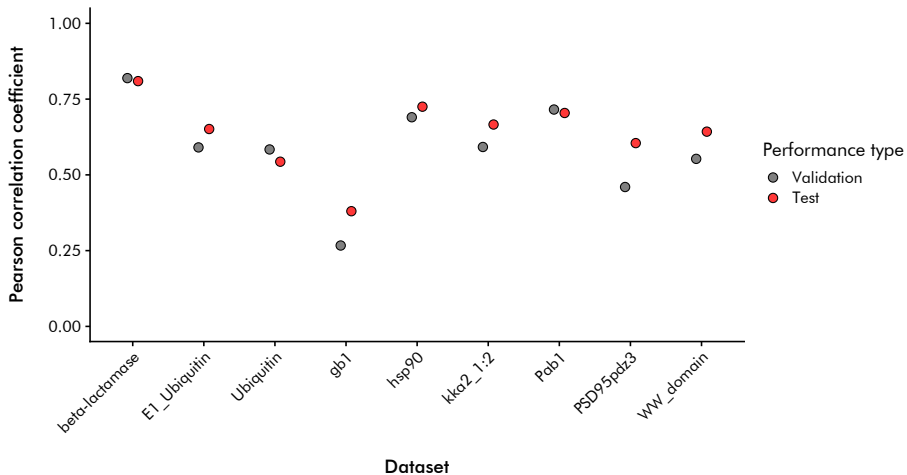
Supplementary Material

Validation and testing performances for the single protein models trained with the naive approach



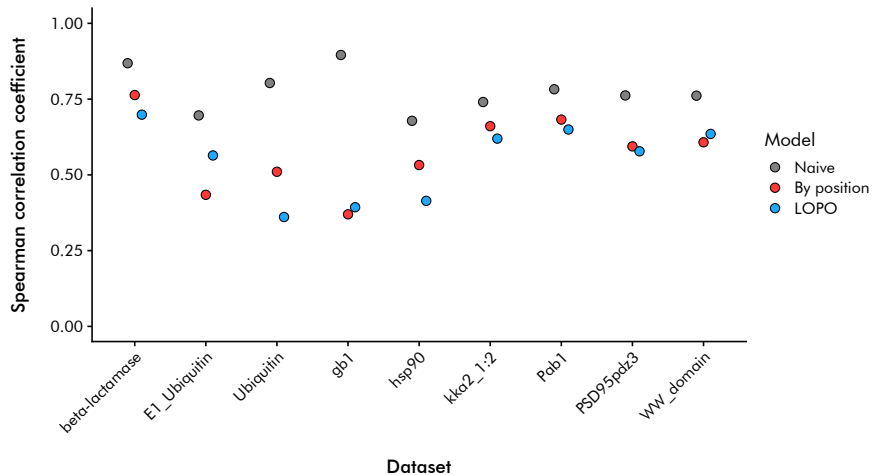
Supplementary Material

Validation and testing performances for the single protein models trained by segregating protein positions



Supplementary Material

Comparison of the performances of single protein models and general models



Confidence intervals in prediction performances

Dataset name	Model	95 % C.I. (Pearson)	95 % C.I. (Spearman)
beta-lactamase	Naïve	0.89 to 0.91	0.86 to 0.88
beta-lactamase	By position	0.79 to 0.83	0.75 to 0.78
beta-lactamase	LOPO	—	0.68 to 0.72
WW_domain	Naïve	0.67 to 0.82	0.70 to 0.84
WW_domain	By position	0.57 to 0.73	0.52 to 0.72
WW_domain	LOPO	—	0.56 to 0.73
PSD95pdz3	Naïve	0.74 to 0.83	0.73 to 0.80
PSD95pdz3	By position	0.55 to 0.67	0.54 to 0.65
PSD95pdz3	LOPO	—	0.53 to 0.63
kka2_1:2	Naïve	0.74 to 0.78	0.72 to 0.76
kka2_1:2	By position	0.65 to 0.69	0.64 to 0.68
kka2_1:2	LOPO	—	0.60 to 0.64
hsp90	Naïve	0.82 to 0.87	0.65 to 0.71
hsp90	By position	0.69 to 0.76	0.50 to 0.57
hsp90	LOPO	—	0.38 to 0.45
Ubiquitin	Naïve	0.75 to 0.83	0.78 to 0.83
Ubiquitin	By position	0.49 to 0.60	0.46 to 0.57
Ubiquitin	LOPO	—	0.30 to 0.43
Pab1	Naïve	0.80 to 0.87	0.75 to 0.82
Pab1	By position	0.65 to 0.76	0.64 to 0.73
Pab1	LOPO	—	0.60 to 0.70
E1_Ubiquitin	Naïve	0.75 to 0.85	0.65 to 0.75
E1_Ubiquitin	By position	0.59 to 0.72	0.36 to 0.51
E1_Ubiquitin	LOPO	—	0.50 to 0.63
gb1	Naïve	0.90 to 0.93	0.88 to 0.92
gb1	By position	0.31 to 0.46	0.29 to 0.45
gb1	LOPO	—	0.32 to 0.47

Supplementary Material

Statistical significance of performance differences. Starred values are significant with Bonferroni correction.

$$\alpha = \frac{0.05}{27} = 0.00185185$$

Dataset name	Model 1	Model 2	p-value
beta-lactamase	Linear regression	Gradient boosted trees	$1 \cdot 10^{-4} *$
beta-lactamase	Linear regression	EVmutation	$1 \cdot 10^{-4} *$
beta-lactamase	EVmutation	Gradient boosted trees	$1 \cdot 10^{-4} *$
WW_domain	Linear regression	Gradient boosted trees	$1 \cdot 10^{-4} *$
WW_domain	Linear regression	EVmutation	$1 \cdot 10^{-4} *$
WW_domain	EVmutation	Gradient boosted trees	$1 \cdot 10^{-4} *$
PSD95pdz3	Linear regression	Gradient boosted trees	$1 \cdot 10^{-4} *$
PSD95pdz3	Linear regression	EVmutation	$1 \cdot 10^{-4} *$
PSD95pdz3	EVmutation	Gradient boosted trees	0.51
kka2_1:2	Linear regression	Gradient boosted trees	0.00
kka2_1:2	Linear regression	EVmutation	0.01
kka2_1:2	EVmutation	Gradient boosted trees	$1 \cdot 10^{-4} *$
hsp90	Linear regression	Gradient boosted trees	$1 \cdot 10^{-4} *$
hsp90	Linear regression	EVmutation	$1 \cdot 10^{-4} *$
hsp90	EVmutation	Gradient boosted trees	0.24

The table continues on the next slide

Supplementary Material

Statistical significance of performance differences. Starred values are significant with Bonferroni correction.

$$\alpha = \frac{0.05}{27} = 0.00185185$$

The table continues from the previous slide

Dataset name	Model 1	Model 2	p-value
Ubiquitin	Linear regression	Gradient boosted trees	$1 \cdot 10^{-4} *$
Ubiquitin	Linear regression	EVmutation	$1 \cdot 10^{-4} *$
Ubiquitin	EVmutation	Gradient boosted trees	$1 \cdot 10^{-4} *$
Pab1	Linear regression	Gradient boosted trees	$1 \cdot 10^{-4} *$
Pab1	Linear regression	EVmutation	$1 \cdot 10^{-4} *$
Pab1	EVmutation	Gradient boosted trees	$1 \cdot 10^{-4} *$
E1_Ubiquitin	Linear regression	Gradient boosted trees	$1 \cdot 10^{-4} *$
E1_Ubiquitin	Linear regression	EVmutation	$1 \cdot 10^{-4} *$
E1_Ubiquitin	EVmutation	Gradient boosted trees	$1 \cdot 10^{-4} *$
gb1	Linear regression	Gradient boosted trees	$1 \cdot 10^{-4} *$
gb1	Linear regression	EVmutation	$1 \cdot 10^{-4} *$
gb1	EVmutation	Gradient boosted trees	$1 \cdot 10^{-4} *$